



# Facile synthesis of bio-based reactive flame retardant from vanillin and guaiacol for epoxy resin

Jingkai Liu<sup>a,b,1</sup>, Jinyue Dai<sup>a,1</sup>, Shuaipeng Wang<sup>a</sup>, Yunyan Peng<sup>a,b</sup>, Lijun Cao<sup>a,b</sup>,  
Xiaoqing Liu<sup>a,\*</sup>

<sup>a</sup> Key Laboratory of Bio-based Polymeric Materials Technology and Application of Zhejiang Province, Ningbo Institute of Materials Technology and Engineering, Chinese Academy of Sciences, Ningbo, Zhejiang, 315201, PR China

<sup>b</sup> University of Chinese Academy of Sciences, Beijing, 100049, PR China

## ARTICLE INFO

### Keywords:

Bio-based flame retardant  
Vanillin  
Guaiacol  
Green solvent  
Epoxy resin

## ABSTRACT

With the purpose to obtain an eco-friendly flame retardant for epoxy resin, a facile method for the synthesis of a bio-based epoxy monomer containing DOPO units (DGEEDB) from lignin-derived vanillin and guaiacol, was presented in this work. During the synthesis process, guaiacol acted as both reactant and solvent. And it could be recycled in situ and re-used as the fresh one. In order to evaluate the flame retardancy of DGEEDB, it was mixed with diglycidyl ether of bisphenol A (DGEBA) and cured with 4,4-diaminodiphenylmethane (DDM). Results showed that, DGEEDB demonstrated a good compatibility with DGEBA, and the mechanical properties of cured resins were obviously improved with the addition of DGEEDB. As expected, the limiting oxygen index (LOI) of cured resin reached 30.2% with the content of phosphorus only 0.67 wt%, in which the weight ratio between DGEEDB and DGEBA was 1:9 (B1D9/DDM). When the weight ratio of DGEEDB to DGEBA was further increased to 2:8 for the B2D8/DDM system, the UL-94 V-0 grade was achieved. Meanwhile, the mechanism of DGEEDB in improving the flame retardancy of cured resin was discussed and revealed. This easily available and eco-friendly DGEEDB proved to be a highly efficient reactive flame retardant for epoxy resin.

## 1. Introduction

Epoxy resins have been commercially available for more than 60 years and became nearly ubiquitous in the fields of aerospace, coating, adhesive and circuit packaging, due to their excellent properties [1–3]. Diglycidyl ether of bisphenol A (DGEBA) is one of the mostly used one, which owns more than 90% market share of all the epoxy resins [4]. However, it still suffers from extremely high flammability and its oxygen index is only about 20%, implying the fast burning speed after lighting [5]. Therefore, how to improve its fire resistance and broaden application field is still a major problem to be solved urgently.

In the last two decades, the incorporation of organic compounds bearing nonmetal boron, halogen, silicon, and phosphorus as well as transition metal [6–10], either as reactants or additives, has been proven to be a quite feasible approach to improve the fire resistance of epoxy resins. Among them, the phosphorus-containing compounds, such as phosphates and 9, 10-dihydro-9-oxa-10-phosphaphenanthrene-10-oxide (DOPO), have attracted much attention due to their non-toxic and

inexpensive features [7,11–13]. Contrast to the addictive flame retardant that is easy to process, the reactive ones have attracted increasing interests in recent years, considering the durable flame retardancy and stable thermomechanical properties of resulted product. However, during the synthesis of a promising reactive flame retardant, not only the complicated chemical synthesis, but also the usage of organic solvents and toxic catalysts is inevitable, which posed a heavy burden on our living environment and threaten humans' health seriously [14,15]. For example, phosphoramidates are frequently used to improve the fire resistance of polymers, which could be synthesized from chlorophosphates through the nucleophilic substitution reaction. However, this reaction is accompanied by hazardous phosphoryl halides and release of chlorine hydride [16]. Atherton-Todd reaction of phosphites could avoid the phosphoryl halides, but still fails to refrain from harmful acid-catching agent and poison solvent [13]. DOPO could be easily chemically attached on the pendant C=C double bond in itaconic acid. However, besides the toxic xylene was necessary for the homogeneous reaction, its LOI index did not exceed 30% until the phosphorus content

\* Corresponding author.

E-mail address: [liuxq@nimte.ac.cn](mailto:liuxq@nimte.ac.cn) (X. Liu).

<sup>1</sup> “Jingkai Liu” and “Jinyue Dai” contributed equally to the writing of this article.

was higher than 2 wt% in the cured system [7]. Xiong et al. designed an addition reaction between DOPO and Schiff base, and the harmful solvents and toxic catalyst were also indispensable [17]. Even if a direct reaction could take place between DOPO and conjugated carbonyl groups, it is also necessary to be refluxed in organic solvent [18]. Meanwhile, according to the principle of green chemistry and owing to the increasing concern on fossil reserve depletion and greenhouse gas emission, synthesis of efficient flame retardant from sustainable building blocks should have greater significance [19,20]. In recent years, using renewable bio-based building block to prepare fire-safe epoxy system has been widely recognized [21,22]. Since the bisphenol A type epoxy currently has an overwhelming market share, the synthesis of high-efficient flame retardants from renewable resources to improve its fire resistance remains a subject of interest.

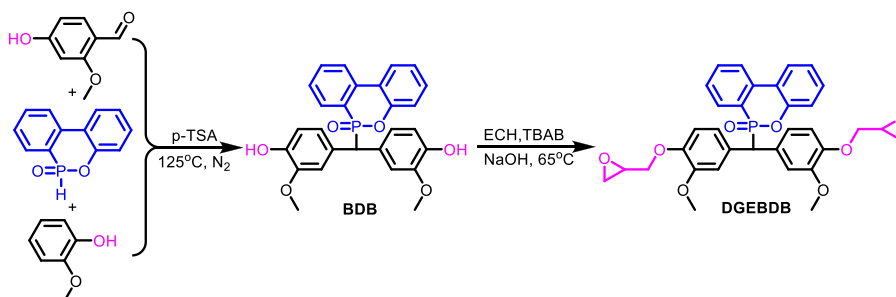
Lignin, which is the second richest natural resource in the world, widely exists in various plants. Up to now, both its abundant availability and success in yielding useful platform chemicals have made it an ideal starting material for the synthesis of bio-based polymers [23,24]. In the last two decades, the preparation of epoxy resins from lignin derivatives, such as vanillin and eugenol, has achieved a series of successes [25–29]. Moreover, a further combination reaction of different lignin derivatives has also shown great potential in the design and synthesis of bio-based thermosets with superior performance [30–33]. Considering the requirements of sustainable development, if the lignin-based compounds could be prepared under environmental-friendly condition, the “green + green” strategy could be implemented.

In this work, with the objective to obtain an efficient flame retardant for epoxy resin from bio-based feedstock, two lignin-derived compounds, vanillin and guaiacol, were taken to combine with DOPO (BDB, Scheme 1) via a straightforward method. And then a DOPO-containing epoxy monomer (DGEGBDB, Scheme 1) was synthesized. The chemical structure and yield of DGEGBDB were carefully characterized, before it was added into DGEBA matrix to evaluate its overall properties in terms of curing behaviors, mechanical strength, thermal stability and fire resistance. We hope this work could bring us a green flame retardant for epoxy through an eco-friendly manner.

## 2. Experimental

### 2.1. Materials

Tetrabutylammonium bromide, 4,4-diaminodiphenylmethane (DDM), vanillin, guaiacol and epichlorohydrin (ECH) were obtained from Aladdin-reagent Co., China. 9, 10-dihydro-9-oxa-10-phosphaphenanthrene-10-oxide (DOPO) were bought from Guangzhou Jinshengji chemical co., Ltd., China. Sodium hydroxide, acetone, and dichloromethane were supplied by Sinopharm Chemical Reagent Co., Ltd., China. Diglycidyl ether of bisphenol A (trade name DER331, abbreviated as DGEBA) with epoxy value around 0.53 was purchased from Dow Chemical Company. All chemicals were all used without further purification.



Scheme 1. Synthesis of BDB and DGEGBDB.

#### 2.1.1. Synthesis of 6-(bis(4-hydroxy-3-methoxyphenyl)methyl)dibenzo [e] [1,2] oxaphosphinine 6-oxide (BDB) and recovery of guaiacol

Vanillin (7.7g, 0.051 mol), guaiacol (37.2g, 0.3 mol), catalytic dose of p-TSA (0.4g, 0.002 mol), and DOPO (10.8g, 0.05 mol) were added into a 250 mL round-bottom glass flask equipped with a reflux condenser. After the mixture was agitated at 100–105 °C for 2 h, the solution underwent an in-situ recovering process by vacuum distillation at the same temperature. The recycled solvent was stored for the next use. After that, tiny amount of acetone was added into the glass flask containing precipitation. Then, the white powder (BDB) was precipitated which was further dried in a vacuum oven (yield: 82.7%). Anal. Calcd for  $C_{27}H_{23}O_6P$ : C, 66.67; H, 5.11; O, 21.34. Found: C, 66.93; H, 5.06; O, 21.45.

#### 2.1.2. Synthesis of bio-based epoxy compound (DGEGBDB)

BDB (40 g, 0.068 mol) was firstly dissolved in ECH (62.8 g, 0.68 mol) with tetrabutylammonium bromide (2 g, 2 wt% of the reaction system) in a 250 mL three-necked flask assembled with constant pressure dropping funnel and a reflux condenser, then the mixture was stirred for 2 h at 75–85 °C with the help of magnetic stirrer. After the solution was cooled down to room temperature, dropwisely adding 20 g of 40 wt% aqueous NaOH (0.2 mol) solution into the mixture and further reacted for another 4 h. An extraction process was conducted and then, the solution in lower levels was distilled by rotary evaporator, in which white precipitation was emerged. DGEGBDB was obtained after being dried in a vacuum oven. Anal. Calcd for  $C_{33}H_{33}O_8P$ : C, 69.61; H, 6.01; O, 19.08. Found: C, 68.23; H, 5.94; O, 19.13.

### 2.2. Preparation of epoxy composites with flame resistance and its curing

Epoxy resins (mole ratio of DGEBA and DGEGBDB was 9: 1, 8: 2, and 7: 3, named as B1D9, B2D8, and B3D7) were well blended with DDM (0.5 times of epoxy group) without solvent. Upon getting the transparent mixture, it was immediately transferred into a heat mold (made by stainless steel) at 120 °C. Then, the curing reaction was conducted at 140–160 °C for 2 h, 180 °C for 2 h, and 200–220 °C for 2 h. Finally, when it was cooled and stayed unused for one day, and the cured material was obtained.

### 2.3. Characterization

$^1H$ ,  $^{13}C$  and  $^{31}P$  nuclear magnetic resonance (NMR) spectra for different systems were collected on a 400 MHz Bruker AVANCE III spectrometer. DMSO or  $CDCl_3$  was used as solvent and tetramethyl silane as internal standard reagent. Elementary analysis was recorded on Organic Element Analyzer (Elementar, Germany), the specimens were tested three times for the accuracy. Dynamic rheological analyzer (DRA) (Anton Paar Physica MCR-301) tests were performed to investigate the rheological behavior of resins containing different content of DGEGBDB. All the samples were not only scanned from 25 to 200 °C using a heating rate of 10 °C/min, but also isothermally heated in a steady-shear mode

at 150 °C for 10 min, with the strain of 0.1% and frequency of 1 Hz, respectively. The diameter of upper plates was 25 mm while the lower one was 50 mm. FT-IR (transmission mode) spectra was conducted on Thermo Nicolet 6700 infrared spectrometer (Thermo-Fisher Scientific). The scanning range was 400–4000  $\text{cm}^{-1}$  and each specimen was scanned 32 times. Before curing reaction, the resin mixtures with different component were observed by Polarizing Microscope (BX51, Japan). The fracture surfaces of cured resins were observed by SEM (EVO18, Germany). Samples were sputtered with a thin layer of gold before testing. The mechanical properties of samples with the dimension of 60 mm  $\times$  10 mm  $\times$  3.5 mm were tested by Universal Mechanical Testing Machine (Instron 5569A). The speed of crosshead is 2 and 5 mm/min for flexural and tensile performances, respectively. All the specimens were evaluated for at least 5 times, and their average was reported. Differential scanning calorimetric (DSC) for evaluating curing reactivity and glass transition temperature were recorded on METTLER TOLEDO-TGA/DSC I. The high purity nitrogen was used as the protecting gas and its flow rate was 20  $\text{mL min}^{-1}$ . The cured resins were tested in the range of 25–300 °C. The heating rate was 10 °C/min for DGEEDB, while the mixed resins were heated by varied rates of 5, 10, 15 and 20 °C/min. Thermogravimetric analysis (TGA) was performed on a Mettler-Toledo TGA/DSC1 thermogravimetric analyzer (METTLER TOLEDO, Switzerland). Nitrogen was used as purge gas (50  $\text{mL/min}$ ), and each sample was heated from 50 to 800 °C. The heating rate was 20 °C/min. DMA curves were collected on a Mettler-Toledo DMAQ800 (tensile mode, frequency of 1 Hz and amplitude of 5  $\mu\text{m}$ ). Each testing sample with bar shape was heated from 30 to 360 °C with the rate of 3 °C  $\text{min}^{-1}$  for three times. The reported results were the averages to guarantee accuracy. Positron Annihilation Lifetime Spectroscopy (PALS) was implemented on a fast-slow coincidence timing spectrometer at Wuhan University. The positrons source time was  $^{22}\text{Na}$  with radiation activity of 0.2  $10^6 \mu\text{Ci}$ . The time resolution in this experiment was 0.23 ns. All the specimens (1.5 cm  $\times$  1.5 cm  $\times$  1 mm) were laid on each side of the source to ensure that the positrons were not penetrated. Each spectrum contains more than  $10^6$  counts. According to the literature [34], the lifetime spectra were analyzed into three positron lifetime components. According to ASTM D3801, UL-94 measurement was conducted on a 5400 vertical burning tester (China). Each specimen with 100 mm  $\times$  13 mm  $\times$  3.2 mm dimension was tested for at least five times. Limited oxygen index (LOI) measurement was conducted following ASTM D2863-97 standard (5801 digital oxygen index analyzers, China). The morphology of carbonaceous layer after UL-94 burning was photographed by SEM. Microscale combustion calorimeter (MCC) was tested on MCC-2. About 5 mg dried sample was recorded from 100 to 700 °C. The heating rate was 1 °C/s under nitrogen stream. X-ray photoelectron spectra (XPS) were obtained on a Kratos Axis Ultra DLD (Kratos, Japan) and the excitation source was Mg K $\alpha$ . In order to improve test accuracy, all the samples were grounded into powders and all the reported energies of spectra were calibrated by C $_{1s}$  set at 284.8 eV.

### 3. Results and discussion

#### 3.1. Synthesis, characterization and solvent recovery

As discussed earlier, in order to obtain the high-efficient flame retardancy, the synthesis of phosphate precursors was usually complicated, and the toxic and harmful solvents were inevitable. Currently, it is urgent for us to avoid or decrease the environmental damage caused by the dangerous reagents during chemical reaction, especially the volatile organic solvent [33,35,36]. In addition, from the environment and energy viewpoints, the chemical synthesis should not only ensure few steps and less pollution, but also a higher yield as well as economical and renewable feedstocks [37]. In this work, we made full use of the combination between bio-based compounds bearing special functional groups (guaiacol and vanillin) and DOPO without addition of any poison solvents and high-risk agents to obtain the bisphenol BDB. Then, BDB

was further converted into a reactive epoxy monomer (DGEEDB) using a simple two-step method widely employed in industry, indicating its great potential for industrialization (Scheme 1).

After optimizing the synthesis condition, the high purity of BDB was confirmed by  $^1\text{H}$  NMR,  $^{13}\text{C}$  NMR, and  $^{31}\text{P}$  NMR (Fig. 1a). It was worth noting that guaiacol served as both reactant and solvent in this reaction, and it could be recovered in situ by vacuum distillation when the reaction was done. We repeated the recovery of guaiacol two times and reused it for the synthesis of BDB. The appearance of fresh and distilled guaiacol as well as the resulted BDB were recorded by digital photos and their chemical structures were identified by  $^1\text{H}$  NMR (Fig. 1b). The  $^1\text{H}$  NMR signals for recovered guaiacol (RG) seemed to be almost the same as those of the original one. And their products possessed nearly the same detection results except the slightly difference in hydroxyl peaks, which was due to the tiny amount of water. The unchanged appearance and structural information here indicated an efficient and feasible recovering and reusing process of guaiacol.

Table 1 shows the yield of RG and BDB produced either in the original or recovered guaiacol under same reaction conditions. It was easy to understand that the weight of RG decreased along with the recycling times, because a part of guaiacol participated in the formation of BDB. Excluding the consumed part in each reaction, the average recovering yield of guaiacol during the recycling processes was as high as 95%. Besides, when the RG was employed for the synthesis of BDB again, without addition of fresh guaiacol, the yield of target product (BDB) was also high up to 82–83%, similar to the yield when fresh guaiacol was used. Thus, it was easy to conclude that a green and facile synthesis method with high yield was used to prepare BDB, where most of guaiacol could be recovered through the in situ distillation under mild condition and reused as the fresh one.

Based on above successful synthesis, the epoxy groups as a common and representative reactive group were grafted onto BDB and a bio-based reactive epoxy monomer, DGEEDB, was obtained. During the synthesis process, not only an expeditious and industrially viable two-step method was adopted, but also the traditional sedimentation based on massive use of long-chain alkane organic compounds was avoided [38]. In order to confirm the success of epoxidation and high purity of DGEEDB, the  $^1\text{H}$ ,  $^{13}\text{C}$  and  $^{31}\text{P}$  NMR, FT-IR spectra was collected. Fig. 2a shows the  $^1\text{H}$  NMR spectrum of DGEEDB, a series of typical signals regarding the epoxy group were noticed, which were marked by a, b, c, f, and g. The  $^{13}\text{C}$  NMR spectrum was taken for further structure identification (Fig. 2b), where the characteristic signals a, b, c, d, and e were the powerful evidence for the successful epoxidation. Due to the diverse aromatic ring in DGEEDB, it was hard to verify the existence of DOPO motif through the  $^1\text{H}$  NMR or  $^{13}\text{C}$  NMR signals, then the  $^{31}\text{P}$  NMR was employed. In Fig. 2c, the peak showing at 32.6 ppm revealed that DOPO motif was successfully attached on the monomer. FT-IR was also used to identify the structure of DGEEDB. As could be seen in Fig. 2d, a series of peaks located at 1238, 1026, 904 and 854  $\text{cm}^{-1}$  were attributed to the epoxy groups [28], and 3064  $\text{cm}^{-1}$  (Ph-H stretching in the DOPO ring), 1592 (P-Ph stretching), 1201 (P=O stretching), and 1142 (P–O–C stretching)  $\text{cm}^{-1}$  stood for DOPO [19]. All these evidences proved that the target product, DGEEDB, was successfully synthesized.

#### 3.2. Processability and compatibility

The different resins were prepared as described in experimental section, the DGEEDB: DGEBA with different ratios (1: 9, 2: 8, and 3: 7, named as B1D9, B2D8, and B3D7, respectively) were blended, in which each system was cured by 4,4-diaminodiphenylmethane (DDM). In general, the curing of epoxy resin undergoes the ring-opening of epoxy group and further polymerization. Resin that can be cured at lower temperature means higher ring-opening activity, and a certain decrease of curing temperature can reduce energy consumption as well as make the processing more convenient [32]. For the sake of evaluating the processability of epoxy resins, it is necessary to investigate its curing

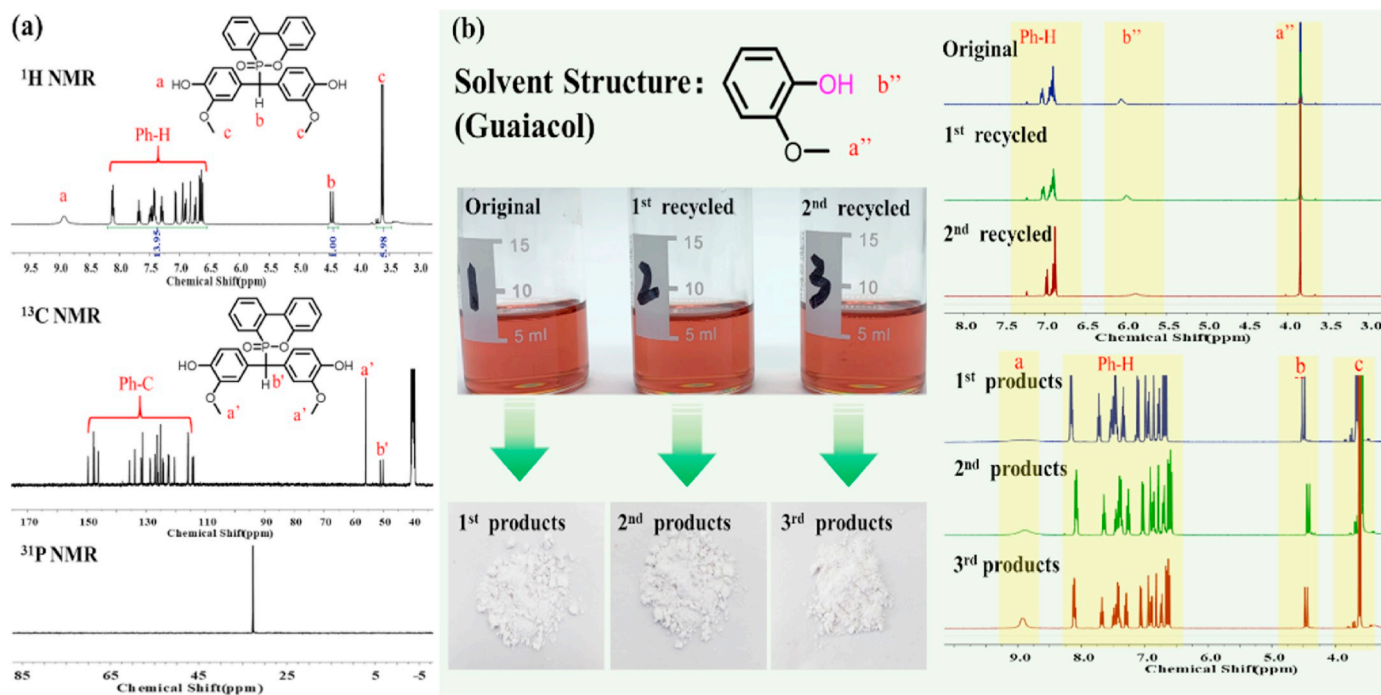


Fig. 1. (a) Chemical structure identification for BDB by <sup>1</sup>H, <sup>13</sup>C, and <sup>31</sup>P NMR; (b) Appearance and structure comparison between the fresh and recycled guaiacol as well as the obtained BDB produced from them.

Table 1

Yield of recovered guaiacol (RG) and BDB produced from RG.

Recycling times	Theoretically unreacted guaiacol (g)	Recovered RG (g)	Yield of RG (%)	Yield of BDB (%)
Original	37.20	–	–	82.74
1	31.03	29.42	94.81	82.14
2	24.17	23.06	95.42	83.57

activity and polymerization temperature [39]. The curing behaviors of different mixture systems (DGEBA/DDM, B1D9/DDM, B2D8/DDM, and B3D7/DDM) under varied heating rates were monitored by DSC. As shown in Fig. 3a, b, c, and d, with the increasing content of DGEBDB, the peak curing temperature of DGEBDB/DDM systems decreased gradually under the same condition. Which indicated that DGEBDB might have a little higher ring-opening activity than that of DGEBA, and the addition of DGEBDB promoted the polymerization of epoxy mixtures.

As we know, the activation energy ( $E_a$ ) is an important parameter for intuitively evaluating the reaction activity. Herein, both Kissinger and Ozawa methods were used to calculate the  $E_a$  of DGEBA/DDM and DGEBDB/DDM systems [40,41]. The Kissinger method can be expressed by the following equation (1):

$$\ln\left(\frac{q}{T_p^2}\right) = \ln\left(\frac{AR}{E_a}\right) - \frac{E_a}{RT_p} \quad (1)$$

where  $q$  is the heating rate ( $^{\circ}\text{C}/\text{min}$ ),  $T_p$  is the peak temperature in curing process (K),  $A$  represents the pre-exponential factor ( $\text{min}^{-1}$ ) and  $R$  serves as the universal gas constant ( $8.314 \text{ J}/\text{mol}\cdot\text{K}$ ).  $E_a$  will be obtained from the average of each curing reaction, the unit of which is  $\text{J}/\text{mol}$ .

As regards the modified Ozawa method, it was delivered by Equation (2):

$$\ln q = \ln\left(\frac{AE_a}{R}\right) - \ln g(\alpha) - 5.331 - 1.052\left(\frac{E_a}{RT_p}\right) \quad (2)$$

Where  $g(\alpha) = \int_0^\alpha \frac{d\alpha}{f(\alpha)} = -\ln(1-\alpha)$  and  $E_a$  can be obtained from the slope of  $\ln q$  against  $T_p^{-1}$ . By linear fitting of transverse coordinates and longitudinal coordinates calculated by Kissinger and Ozawa formula, the  $E_a$  and  $\ln A$  of both DGEBA/DDM and DGEBDB/DDM can be obtained from the slope and intercept of resultant lines in Fig. 3e and f. As could be seen in Table 2, neither  $E_a$  nor  $\ln A$  of DGEBDB/DDM and DGEBA/DDM showed obvious difference. However, on the one hand, there was indeed a visible effect on lowering the polymerization temperature when the content of DGEBDB was increased (Fig. 3a–d), indicating that the addition of DGEBDB slightly accelerated the polymerization of DGEBDB and DGEBA mixture, instead of hindering. On the other hand, the very close value of  $E_a$  enabled both DGEBA and DGEBDB to copolymerize well under the same curing conditions, which was beneficial to the formation of a homogeneous and compatible system.

As an ideal reactive flame retardant for epoxy, besides its capability to improve the fire resistance, it should be well compatible with the matrix and pose negative impact on the properties of target composites as little as possible [9]. Accordingly, we first observed whether the mixed systems were homogeneous or not by both macro and micro aspects. As shown in Fig. 4a, all the mixtures were homogeneous, transparent and pale-yellow liquids, indicating the good compatibility between DGEBDB, DGEBA and DDM. This result was further proved by the polarized microscope photograph for B3D7/DDM system showing in Fig. 4b, in which neither tiny particles nor undissolved substance was observed, implying the good dissolution of DGEBDB in the DGEBA matrix again. DSC and dynamic rheological analyzer (DRA) were used to study the thermal behavior of DGEBDB during the possible heating process. As shown in Fig. 4c, it displayed a very sharp melting peak at  $123.1^{\circ}\text{C}$  without any other enthalpy change, suggesting its high-purity again. In addition, we also monitored the viscosity change of DGEBDB starting from the temperature near its melting point. Its viscosity remained nearly unchanged after a sharp decline around  $120^{\circ}\text{C}$ , which indicated the stability of DGEBDB and only a typical melting process took place on the heating-up case.

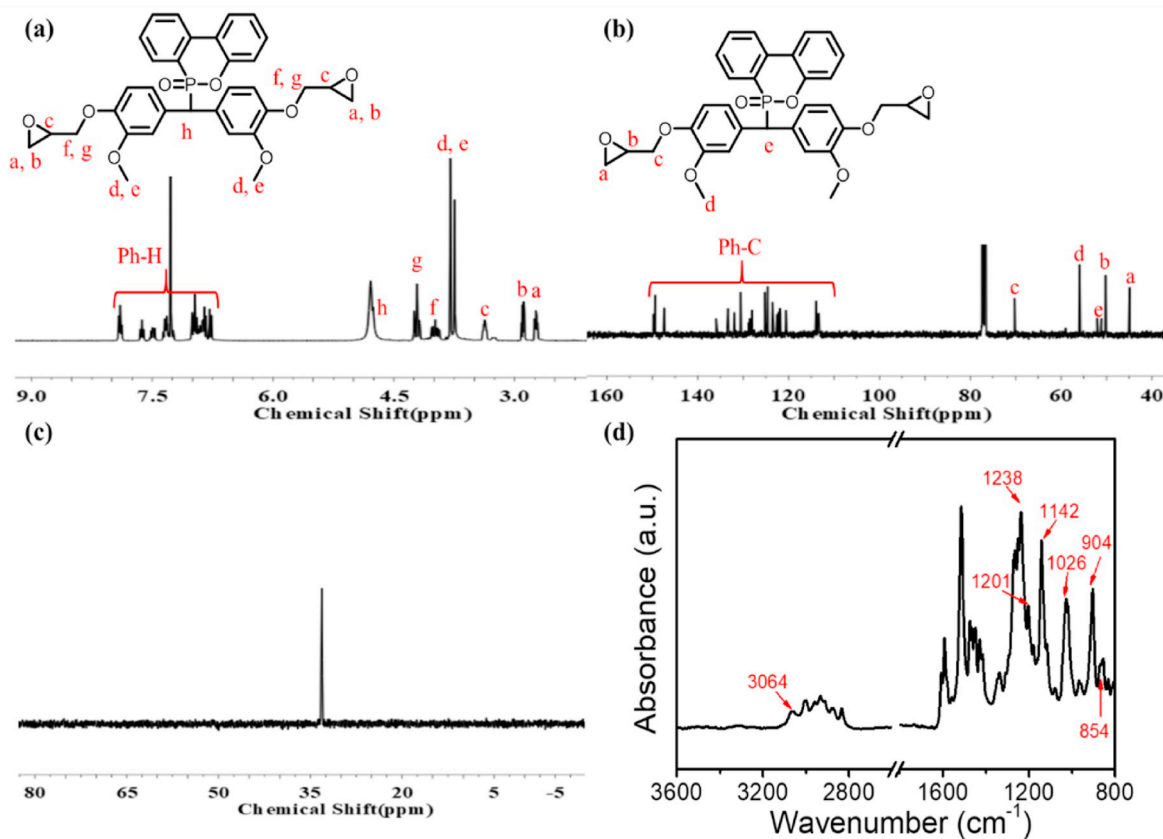


Fig. 2.  $^1\text{H}$  NMR (a),  $^{13}\text{C}$  NMR (b), and  $^{31}\text{P}$  NMR (c) spectra of DGEbDB; FT-IR spectra from 800 to 3600  $\text{cm}^{-1}$  of DGEbDB (d).

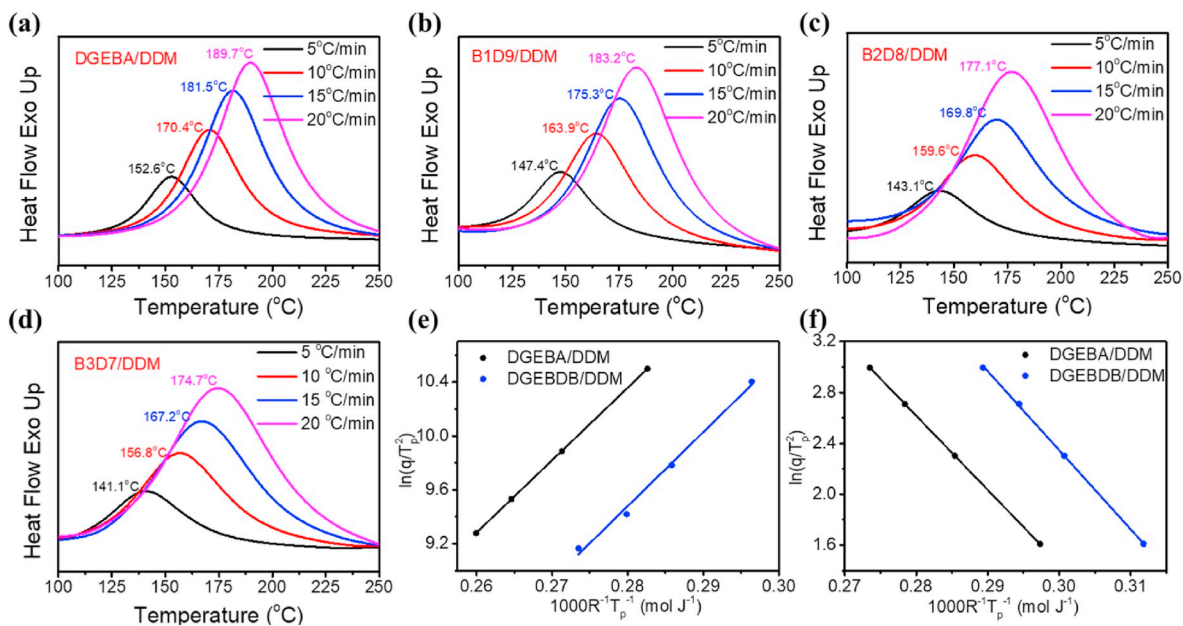


Fig. 3. DSC curves for DGEBA/DDM (a), B1D9/DDM (b), B2D8/DDM (c), and B3D7/DDM (d) at different heating rates; The related fitting curves for DGEBA/DDM and DGEbDB/DDM based on Kissinger (e) and Ozawa (f) equations.

**Table 2**  
Curing kinetics data of different systems.

Specimens	Heating rates ( $q$ ) ( $^{\circ}\text{C min}^{-1}$ )	$T_p$ (K)	$E_a$ (kJ/mol)		$\ln A$	
			Kissinger	Ozawa	Kissinger	Ozawa
DGEBA/ DDM	5	425.6	53.80	58.14	14.45	15.78
	10	443.5				
	15	454.6				
	20	462.7				
DGEBDB/ DDM	5	405.8	54.91	58.85	15.64	15.87
	10	419.9				
	15	429.8				
	20	439.3				

<sup>a</sup> The dimension of  $A$  is  $\text{min}^{-1}$ , and  $\alpha$  was 0.5.

Processing window is usually used to assess resin's workability. Resin with appropriate processing window is available for the resin transfer molding (RTM), which is usually taken to prepare polymeric composites and developed rapidly in recent years with reduced cost and improved efficiency [42,43]. In general, as for the resin suitable for RTM, its viscosity should be stably below 1 Pa s at least for half an hour at the processing temperature [44]. Fig. 4d displayed the relationship of viscosity and temperature for DGEBA/DDM, B1D9/DDM, B2D8/DDM and B3D7/DDM, respectively. It showed that, from 25 to 150  $^{\circ}\text{C}$ , their viscosities remained very stable and as low as 1 Pa s. When the

temperature was further increased, the sharp rise in their viscosities, indicating the rapid curing reaction, was observed. This result corresponded to above DSC results very well. For further processability investigation, B3D7/DDM system was taken as an example and its viscosity change along with time at different temperature (80, 90, 100, and 110  $^{\circ}\text{C}$ ) was depicted in Fig. 4e. As expected, its viscosity was increased faster at a higher temperature. And when the processing temperature was set at 80  $^{\circ}\text{C}$ , the B3D7/DDM system could maintain its viscosity below 1 Pa s for more than 30 min. Based on the results in Fig. 4d, it was reasonable to believe that, at the temperature lower than 80  $^{\circ}\text{C}$ , its viscosity below 1 Pa s would last longer, which indicated that there was long enough time to conduct the resin injection during RTM process [45]. Besides, when the temperature was increased up to 150  $^{\circ}\text{C}$ , all the resin systems reached gel point (viscosity of  $10^3$  Pa s) only in several minutes (Fig. 4f), indicating their high curing activities. All these results highlighted that DGEBDB was well compatible with DGEBA matrix and hardly on negative impact on its processability was detected. The highly efficient RTM was applicable for the processing of DGEBDB/DGEBA mixtures.

Before thermal and mechanical properties evaluation, it is necessary to ensure that the epoxy resin is fully cured. Accordingly, FT-IR measurement for the different epoxy mixtures after curing reaction was conducted. As shown in Fig. 5a, all the systems exhibited similar FT-IR curves. And compared with the FT-IR spectra in Fig. 2d, which showed very strong characteristic signals for epoxy group at 904 and

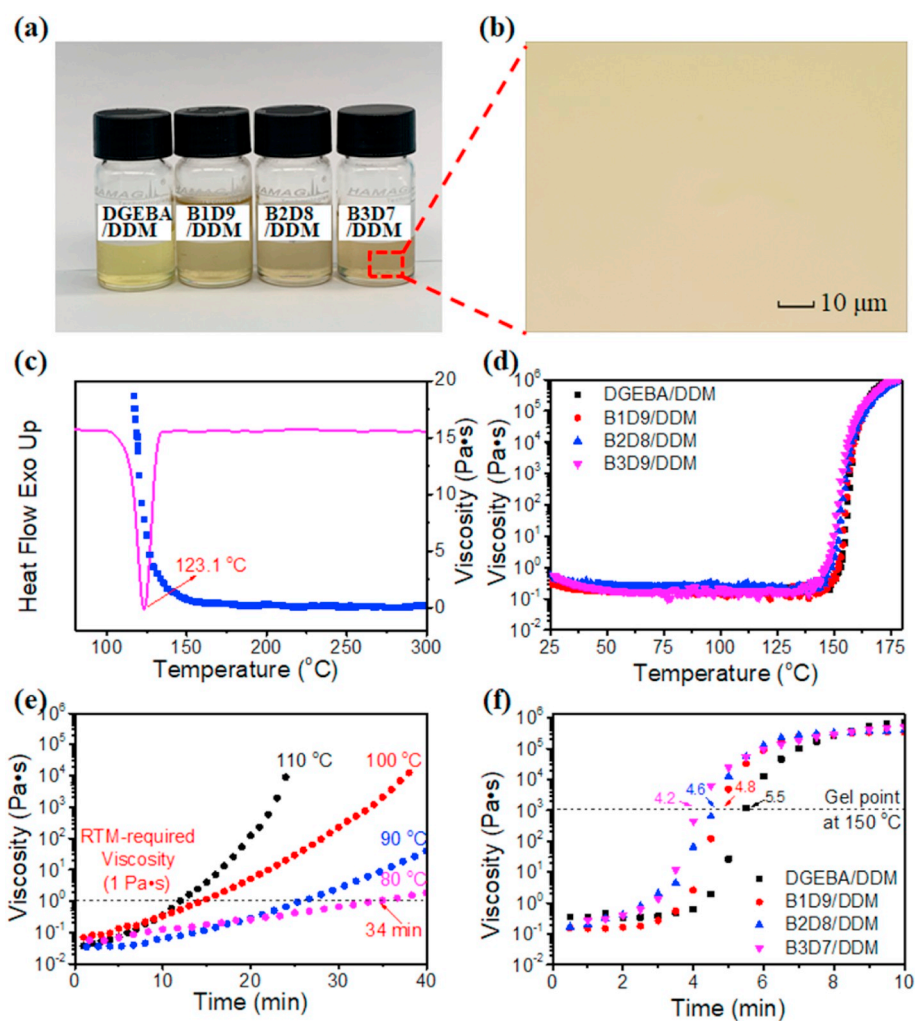


**Fig. 4.** Compatibility investigation on DGEBDB/DGEBA mixtures: macroscopical scale (a) and polarizing microscope image (b); Non-isothermal DSC and related viscosity curves determined by DRA for DGEBDB(c); Viscosity as a function of temperature (d) and viscosity-time curves at different temperatures for B3D7/DDM (e), viscosity-time curves for all the DGEBDB/DGEBA mixtures isothermally recorded at 150  $^{\circ}\text{C}$  (f).

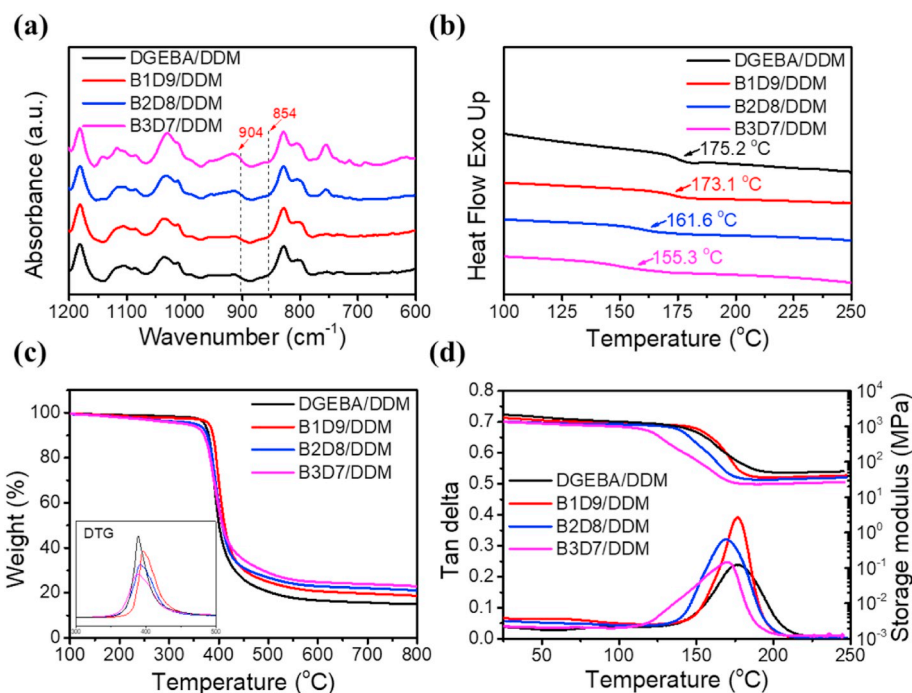


Fig. 5. FT-IR spectra (a), DSC curves (b), TGA and DTG curves (c), and  $T_g$  determined by DMA (d) for all the cured resins in this work.

854  $\text{cm}^{-1}$ , the bonds for epoxy group in Fig. 5a could be regarded as completely disappeared, indicating the full curing reaction in some extent. In addition, this result also indicated that, instead of a physically mixed additive, DGEEDB was chemically bonded together with DGEBA.

### 3.3. Thermal and mechanical performance

The thermal and mechanical properties of all the materials were estimated by DSC, TGA and DMA (Fig. 5). The related values including  $T_g$  (temperature at glass transition),  $T_{d10\%}$  (10% degradation occurred temperature),  $T_{max}$  (temperature at which the fastest thermal degradation was observed), and char yield at 800 °C were collected in Table 3. As shown in Fig. 5b, the  $T_g$  of DGEBA/DDM determined by DSC curve was about 175.2 °C, which was similar to the previously reported value [38], implying that the curing conditions and results in this work were reasonable and credible. With the addition of DGEEDB, a slight decrement in the  $T_g$  value for cured resin was noticed, from 173.1 °C for B1D9/DDM to 155.3 °C for B3D7/DDM. It is known that the  $T_g$  of epoxy material is closely related to the cross-link density of network and the rigidity of chain segment. Generally, DOPO, as a rigid group, should have a positive contribution to the  $T_g$  [45]. However, the addition of DGEEDB bearing DOPO led to a decreased  $T_g$  here. The reason might be that DOPO was served as a pendent group and its contribution to  $T_g$  was negligible, while the cross-link density of cured resins might be lowered. Fig. 5c shows the TGA curves for the cured resins. Based on the data listed in Table 3, it was found that among the three phosphorus-containing systems,  $T_{d10\%}$  showed a decreasing trend with the increasing content of DGEEDB, the  $T_{d10\%}$  for B1D9 was a little higher than those for both B2D8 and B3D7 systems. The reason might be

ascribed to that DGEEDB is a monomer containing multiple aromatic rings and easily decomposed chemical bonds (P–O and P–C), in which the aromatic units can improve its thermal stability while the relative weak bonds will reduce the initial degradation temperature. It was the synergistic effect that resulted in their differences in  $T_{d10\%}$  values. As for the  $T_{max}$  determined by DTG curves inserted in Fig. 5c, all the systems exhibited a one-stage degradation process and a similar trend as  $T_{d10\%}$ . In addition, a smaller peak intensity and a lower  $T_{max}$  were noticed for the DGEEDB richer systems, which showed the similar results as some nonflammable epoxy systems under nitrogen atmosphere [46], suggesting that the earlier char stabilization and the lower weight loss rate. And this result was also attributed to the synergistic effect of multiple aromatic rings and easily decomposed P–O and P–C bonds. What should be emphasized here was that the char yield was obviously increased with the introduction of DGEEDB. As for DGEBA/DDM, the char yield was only 14.9%, while it was gradually increased to 23.3% for B3D7/DDM. Sometimes, the char yield of thermoset is related to its flame retardancy. The high char yield represents a lower flammability, and the systematical investigation on their flame retardant properties will be conducted in the following section.

Fig. 5d illustrates the DMA curves of all the cured systems. Obviously,  $T_g$  determined by the peak temperatures of  $\tan \delta$  curves were a little higher than the ones obtained from the DSC curves in Fig. 5b. This was reasonable due to the difference between DMA and DSC measurement. Notably, the single glass transition peak in Fig. 5d clearly supported that DGEEDB unit was compatible with DGEBA after curing reaction except for the slightly asymmetric profile of  $\tan \delta$  peak for the B3D7/DDM system. That indicated a slight heterogeneity probably caused by the more rigid structure of DGEEDB, which might inhibit the

Table 3  
 $T_g$  and thermal degradation behaviors for all the cured systems.

Samples	$T_g$ based on DSC (°C)	$T_g$ based on DMA (°C)	$T_{d10\%}$ (°C)	$T_{max}$ (°C)	Char yield at 800 °C (%)	$E'$ at RT (MPa)	$\nu_e/10^3$ (mol/m <sup>3</sup> )
DGEBA/DDM	175.2	177.8	379.6	385.8	14.9	2287	8.8
B1D9/DDM	173.1	176.4	385.5	395.9	19.1	1833	7.0
B2D8/DDM	161.6	169.2	376.1	392.1	21.2	1621	6.3
B3D7/DDM	155.3	168.9	375.3	389.9	23.3	1575	5.2

molecular motions during curing reaction. The storage modulus ( $E'$ ) and crosslinked density ( $\nu_e$ ) obtained from DMA results were collected in Table 3, in which  $\nu_e$  was calculated by rubber elasticity theory (equation (3)):

$$\nu_e = E' / 3RT \quad (3)$$

where the  $E'$  in this equation is the corresponding storage modulus of the polymer in the rubbery plateau region,  $R$  is the gas constant and  $T$  ( $T_g + 30$ ) is the absolute temperature. As could be seen, the storage modulus at room temperature decreased with the increasing content of DGEEDB, which was attributed to the decreasing cross-link density, while the calculated  $\nu_e$  values showed a good support for this deduction.

In order to make a further confirmation of compatibility, SEM images for the fracture surface of all the cured systems are shown in Fig. 6. Besides the typical features for brittle fracture were observed, the uniformly fractured surface without any domains represented a single-phase and homogeneous cross-linked network, which also indicated the good compatibility between DGEEDB and DGEBA after curing reaction [47].

Fig. 7a and b show the tensile and flexural properties of all the cured resins. Both the tensile strength and modulus were increased with the addition of DGEEDB. DGEBA/DDM system showed an average tensile strength and modulus of 74.1 and 2375.6 MPa, respectively. For B1D9/DDM, B2D8/DDM and B3D7/DDM, their tensile strength was 84, 87 and 91 MPa, with the tensile modulus of 2640, 2771, and 2854 MPa, respectively (Fig. 7a). Their flexural performance showing in Fig. 7b also illustrated an almost the same variation trend as the tensile properties. From DGEBA/DDM to B3D7/DDM, an obvious increment in flexural modulus and strength was observed. Especially, the flexural modulus of B3D7/DDM was increased by 54% compared with that of DGEBA/DDM, which should be attributed to the higher rigidity of DGEEDB.

As is known, modulus reflects the deformation resistance of material, which mainly depends on the features and density of chemical bond along with the intermolecular force, while the free volume directly affects the stuffing density of chemical bonds [48,49]. In a simple term, there is usually a negative correlation between the free volume and mechanical properties. Accordingly, the deep reason for the improvement of modulus was investigated with the help of PLAS in the way of calculating free volume. Generally, in PLAS measurement, there will be para (p-Ps) and ortho positronium (o-Ps) when positrons and electrons

collide, which are only effective to the amorphous polymers. Three relative parameters corresponded to  $\tau_1$  (para positronium),  $\tau_2$  (free positron) and  $\tau_3$  (ortho positronium) were produced after annihilation occurs, and the longest-lived  $\tau_3$  reflected the free volume. Furthermore, the radius ( $R$ ) of free volume can be obtained by  $\tau_3$  via Eq. (4).

$$\tau = \frac{1}{2} \left[ 1 - \frac{R}{R + \Delta R} + \left( \frac{1}{2\pi} \right) \sin \left( \frac{2\pi R}{R + \Delta R} \right) \right]^{-1} \quad (4)$$

$$FFV = CV_F I_3 \quad (5)$$

In which,  $\Delta R$  is the electron layer with the thickness of 0.1656 nm [50]. Fig. 7c shows the  $\tau_3$  values and  $R$ . As could be seen, from DGEBA/DDM to B3D7/DDM,  $\tau_3$  was decreased with the increasing content of DGEEDB, and so did  $R$ . Fractional free volume ( $FFV$ ) represents the content of free volume in polymers, as shown in Eq. (5), where  $C$  (value is  $0.0018 \text{ \AA}^{-3}$ ) is an arbitrarily scaling factor for a spherical cavity and  $V_F = 4\pi R^3/3$  serve as the average value of free volume. It's clear that  $R$  and  $I$  were two physical quantity related to  $FFV$ . As shown in Fig. 7d, the calculated  $FFV$  values followed the descending order from DGEBA/DDM to B3D7/DDM. By comparing the chemical structures of DGEBA and DGEEDB, it was easy to conclude that the pendent DOPO group and methoxyl attached on benzene ring in DGEEDB should be responsible for the  $FFV$  reduction after the addition of DGEEDB. In the curing process, these side groups were more likely to fill the voids, therefore both the number and size of these voids will be reduced. In other words, the lower  $FFV$  meant a larger filling density due to the presence of more side groups in the DGEEDB richer systems, which had a positive contribution to the modulus of cured resins.

### 3.4. Flame retardancy

In order to systematically investigate the fire safety of cured resins with the introduction of DGEEDB, both UL-94 vertical-burning experiment and limiting oxygen index (LOI) test were conducted. And the related values were collected in Table 4. The UL-94 vertical burning test was thought to be a visual method for the combustion characterization. As shown in Fig. 8a, DGEBA/DDM demonstrated visible flammability, which was almost entirely burned out in 60 s. In contrast, the cured resins containing DGEEDB did not show an intensive combustion. After ignition, even the burning B1D9/DDM, in which the mole ratio of DGEEDB to DGEBA was only 1:9 and the phosphorus content was 0.67

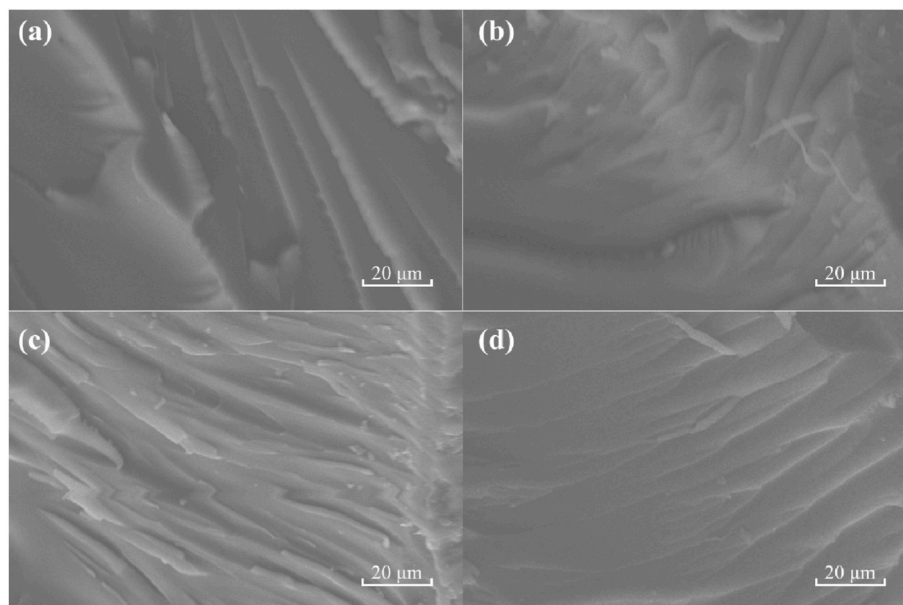


Fig. 6. SEM images for the fracture surfaces of different cured systems: DGEBA/DDM (a), B1D9/DDM (b), B2D8/DDM (c), and B3D7/DDM (d).



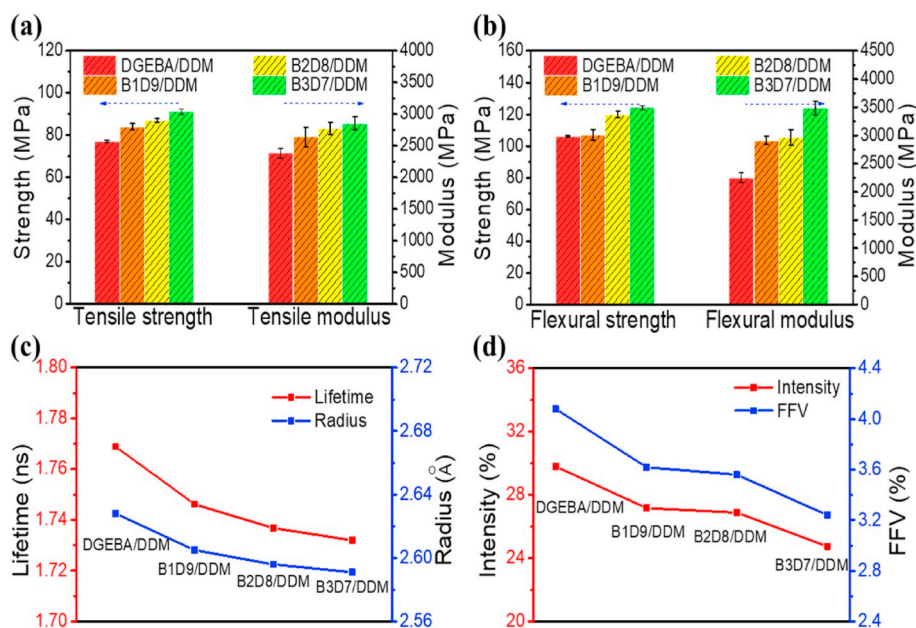


Fig. 7. Mechanical properties of all the cured resins: tensile strength and tensile modulus (a); flexural strength and flexural modulus (b); PALS results for the fully cured resins: o-Ps lifetime and R of free volume holes (c); o-Ps intensity (indicative of hole amount) and fractional free volume (FFV) (d). (Dotted lines were plotted here only for easy observation.)

Table 4  
UL-94 burning and LOI results for cured systems.

Specimens	Phosphorus content (%)	LOI (%)	UL-94		MCC			
			$t_1 + t_2$ (s)	UL-94	Flaming drips	$T_p$ (°C)	HRR (J/g.K)	THR (kJ/g)
DGEBA/DDM	0	24.2		NR	yes	397.3	724	25.1
B1D9/DDM	0.67	30.2	11.4	V-1	none	385.7	500	22.1
B2D8/DDM	1.27	32.4	4.7	V-0	none	380.7	386	20.5
B3D7/DDM	1.81	33.4	1.9	V-0	none	386.4	348	18.4

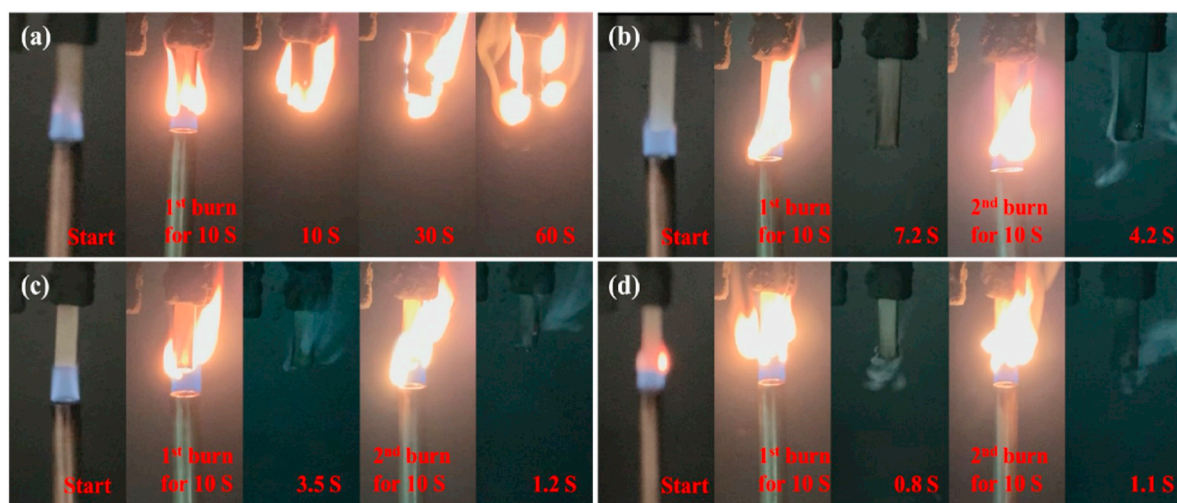


Fig. 8. Digital photographs for UL-94 test of different systems: (a) DGEBA/DDM, (b) B1D9/DDM, (c) B2D8/DDM, and (d) B3D7/DDM.

wt%, could self-extinguish in 7.2 s. When it was ignited for the second time, its self-extinguishing time was only 4.2 s. With the increasing content of DGEBDB in the cured systems, from B2D8/DDM to B3D7/DDM, the flame was getting smaller and the value for  $t_1+t_2$  was shortened from 4.7 to 1.9 s, the phosphorus content of the former one was as low as 1.27 wt% while that of the latter one was only 1.81 wt%. In addition, no flaming drips from the burning samples were observed

during the combustion. As for the LOI measurement, the flammable DGEBA/DDM system showed low LOI of 24.2%. While the LOI was increased with the content of DGEBDB in the cured systems. For B3D7/DDM, whose phosphorus was calculated to be only 1.81 wt%, its LOI was as high as 33.4%. Summarily, DGEBA/DDM showed no combustion grade (UL94 NR). However, both B2D8/DDM and B3D7/DDM were rated as the highest flame-retardant grade (UL-94 V0). Compared with

previously reported results [18,51], the higher efficiency and advantages of DGEEDB in improving the fire-resistance of epoxy resin was indubitable. For example, Artner and his coworkers [51] once synthesized a DOPO-containing reactive flame retardant, the LOI of the resulting resin could up to 48%, but it failed to achieve UL-94 V-0 grade. Wang [18] reported a flame retardant epoxy monomer with properties similar to DGEEDB, but the phosphorus content was higher than 7 wt %.

Microscale combustion calorimetry (MCC) can not only quantify the flammability of samples by specific data, so as to more accurately compare the flame retardancy of different samples, but also has the advantage of small sample requirement. Herein, MCC was taken to evaluate the combustion and heat release of decomposed gases within a certain temperature range, in which the specific heat release rate (HRR) and total heat release (THR) of all the cured resins were recorded. Fig. 9 presents the typical MCC curves for THR vs. temperature as well as HRR vs. temperature, and the values for THR, HRR, and peak heat release temperature ( $T_p$ ) were collected in Table 4. Results showed that all the cured systems demonstrated  $T_p$  in the temperature range of 386–397 °C. Compared with the  $T_{max}$  (temperature at which the fastest degradation occurred) obtained from TGA curves in Fig. 5c, a little deviation was observed for the same specimen, which might be caused by the principle difference between MMC and TGA. With the increasing content of DGEEDB, the value of HRR at  $T_p$  for different cured resins showed great difference. From DGEBA/DDM to B3D7/DDM, HRR was decreased from 724 to 348 J/g.K, showing a reduction by 52%. Meanwhile, the THR also showed a downward trend with the introduction of DGEEDB. All the results suggested that the flammability of B1D9/DDM, B2D8/DDM, and B3D7/DDM were considerably lower than that of DGEBA/DDM.

It is well recognized that a deep insight into the mechanism of fire-resistance will be helpful for us to optimize the flame-retardant modification process. As we know, DOPO and its derivatives generally act in gas phase by reducing the free radical, and some of them with special structure can play a positive role in the gas and condensed phase

simultaneously [52]. Considering the multi-aromatic structure of DGEEDB, it is not difficult to speculate its positive influence in charring. Thus, important information could be obtained by investigating the carbonaceous structure of combusted resins, which was recorded carefully and photographed by SEM (Fig. 10). Based on the preliminary observation on the morphology of char residues, the higher flame retardant efficiency of DGEEDB containing systems was partly attributed to the char layers in the condensed phase [53,54]. From Fig. 10a, it was seen that the char residue on the surface of burnt DGEBA/DDM was loose and porous. After the addition of DGEEDB, a denser and flatter carbon layer was formed on the surface of burnt resins (Fig. 10c and d), which effectively contributed to heat insulation, oxygen barrier and inner material protection [55,56]. In addition, the relatively high integrated char structures of cured B1D9/DDM, B2D8/DDM and B3D7/DDM during combustion could maintain the original shape of resins, then slow down the release of combustible gas and the spread of combustion rate [57]. When carefully look at the higher resolution pictures inserted in Fig. 10, a small amount of fluffy char on the surface of combusted B1D9/DDM was observed (Fig. 10b). For B2D8/DDM system, the denser carbon layer was formed, and no fluffy char was found on the surface of residues (Fig. 10c). As regards B3D7/DDM system, the carbon layer on the surface of burnt material was quite flat, which was in a good agreement with its best flame-retardant properties. It concluded that not only DGEEDB played an important role in condensed-phase flame-retardant, but also the observed morphologies could partly explain the non-flammability of the cured resins.

The involved elements' contents in the exterior carbon layer of burnt DGEBA/DDM, B1D9/DDM, B2D8/DDM, and B3D7/DDM were analyzed by XPS (Fig. 11), and the related results are displayed in Table 5. It showed that the content of phosphorus element in them were 0, 0.18, 0.43, and 1.77%, respectively. Accordingly, where the oxygen content was also increased from 11.35% for the DGEBA/DDM system to 17.45% for the B3D7/DDM as well, this was due to the fact that the phosphorus element in the surface char residues remained more oxygen atoms in the form of pyrophosphate and/or polyphosphate (133.6 eV,  $P_{2p}$ ; 191.2 eV,  $P_{2s}$ ) [58]. As for the cured DGEBA/DDM, the  $C_{1s}$  peak was split into three typical bands with the binding energies of 284.6, 286.1, and 288.6 eV (Fig. 11c), in which the predominant band showing at 284.6 eV was corresponded to C–H, C–C and C=C in aliphatic or aromatic species, and the other two bands were assigned to C–N/C–OH/C–O–C and O=C, respectively [19,59]. Fig. 11d, e, and f were the split  $C_{1s}$  peaks for cured B1D9/DDM, B2D8/DDM, and B3D7/DDM. After adding flame retardants, the proportion of 284.6 eV area increased slightly, meaning that more carbon was retained after the material burned possibly due to contribution of DGEEDB. In addition, the new peak at 290.8 eV, indicating the presence of C–P bond, emerged in the systems containing DGEEDB [12]. These results suggested an important role of DGEEDB in enhancing the fire-safety of cured DGEBA.

#### 4. Conclusions

Two lignin-derived compounds, vanillin and guaiacol, were successfully combined with DOPO, via a facile and green reaction without extra organic solvents, where guaiacol served as not only a reagent, but also a good solvent. In addition, guaiacol could be well recovered in situ and reused. The synthesized BDB was efficiently converted into an epoxy monomer DGEEDB using the method widely employed in industry. DGEEDB had a good compatibility with the commercial epoxy resin DGEBA, then they were mixed with different ratios and DGEEDB showed great potential in serving as a reactive fire-resistant with superior flame retardation properties agent for DGEBA. Besides the high curing reactivity and excellent processability of DGEEDB, good mechanical and thermal properties of cured resins, DGEEDB promoted the flame-retardant-grade of highly flammable cured DGEBA to UL-94 V-0 with the phosphorus content of only 1.27 wt%. Summarily, a bio-based, reactive flame retardant for epoxy was successfully synthesized in a

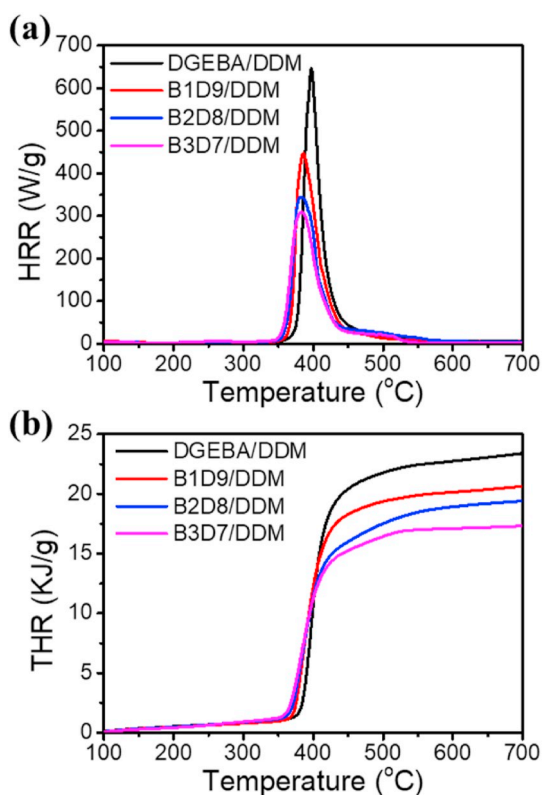


Fig. 9. MCC curves of four systems: specific heat release rate (HRR) vs. temperature (a) and total heat release (THR) vs. temperature (b).

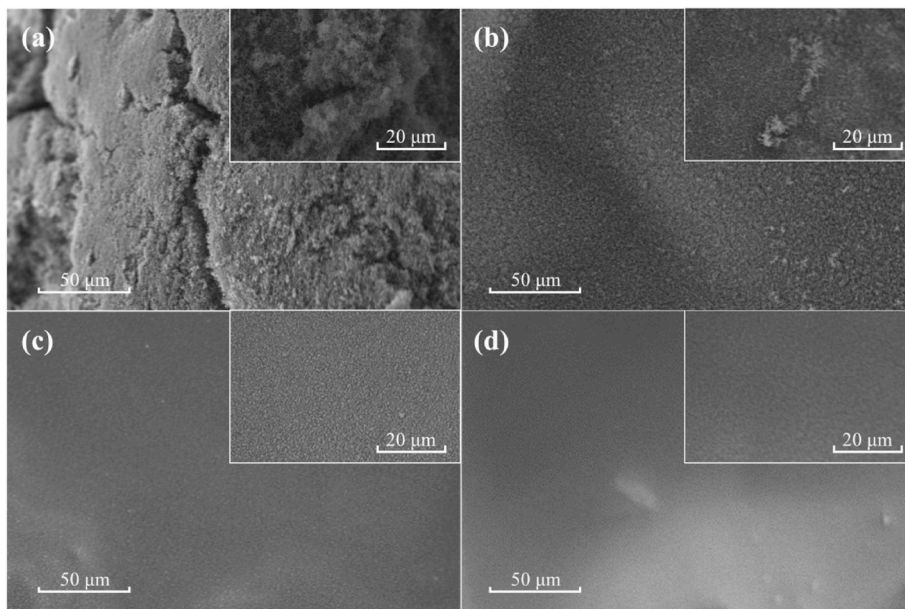


Fig. 10. SEM graphs of exterior carbon layers for the burned: DGEBA/DDM (a), B1D9/DDM (b), B2D8/DDM (c), and B3D7/DDM (d).

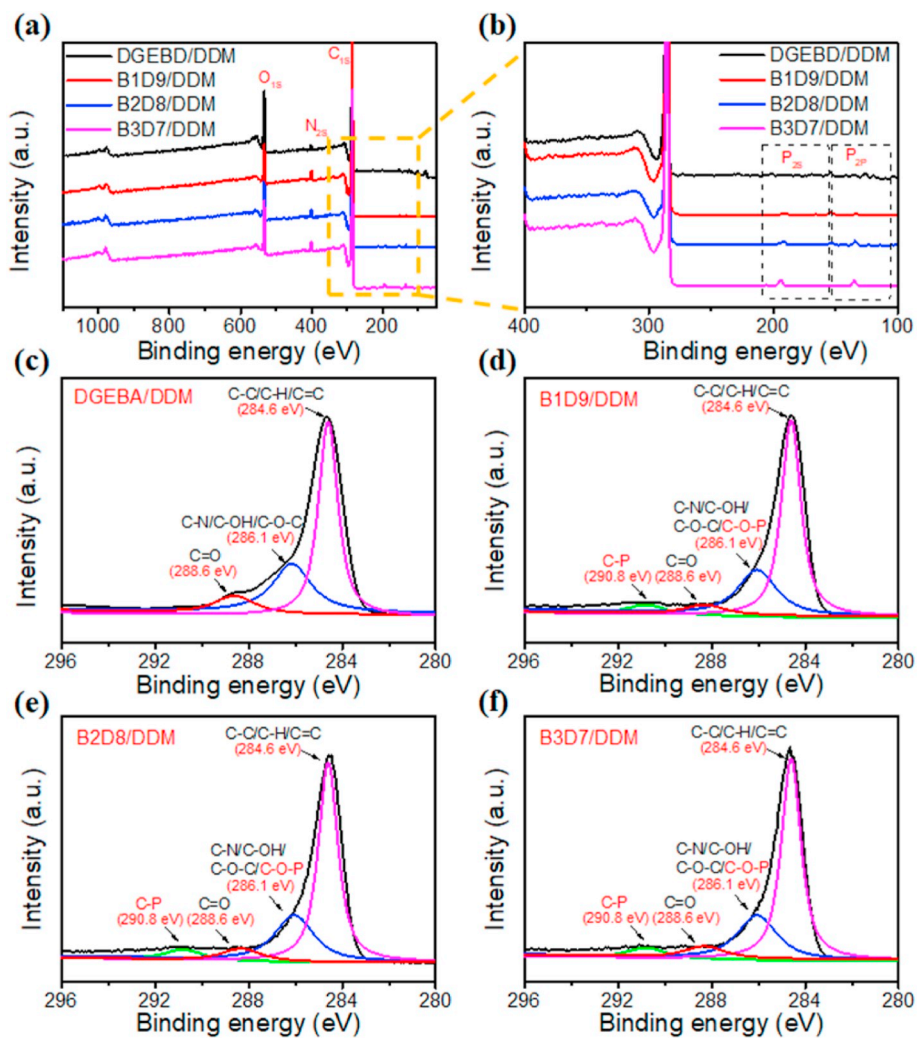


Fig. 11. XPS spectra for the surface of residual char layers of burnt resins: overall spectra (a); enlarged picture containing peaks for  $P_{2s}$  and  $P_{2p}$  (b); peak splitting for  $C_{1s}$  signals of DGEBA/DDM (c), B1D9/DDM (d), B2D8/DDM (e), and B3D7/DDM (f).

Table 5

Elemental contents on the surface of residual char layers based on XPS.

Element	Samples			
	DGEBA/DDM	B1D9/DDM	B2D8/DDM	B3D7/DDM
C (wt %)	84.38	80.98	76.79	75.76
N (wt %)	4.27	5.13	5.06	5.02
O (wt %)	11.35	13.71	15.26	17.45
P (wt %)	—	0.18	0.43	1.77

green solvent, which showed great potential to make the epoxy resins or related composites safer and greener. However, the employed epichlorohydrin is still toxic and petroleum-based in this work. In the future, if all the reagents and process could be eco-friendly, it will be more significant.

#### Declaration of competing interest

The authors declare no competing financial interest.

#### CRediT authorship contribution statement

**Jingkai Liu:** Methodology, Formal analysis, Writing - original draft. **Jinyue Dai:** Methodology. **Shuaipeng Wang:** Formal analysis. **Yunyan Peng:** Resources. **Lijun Cao:** Conceptualization. **Xiaoqing Liu:** Supervision, Writing - review & editing.

#### Acknowledgement

This work was supported by Chinese Academy of Sciences (Key Research Program KFZD-SW-439), Zhejiang Provincial Natural Science Foundation of China (No LR20E030001), National Natural Science Foundation of China (No U1909220), National Ten Thousand Talent Program, Zhejiang Ten Thousand Talent Program, Chinese Postdoctoral Science Foundation (2018M642499).

#### References

- [1] May C. Epoxy resins: chemistry and technology. Routledge; 2018.
- [2] Zhang Q, Molenda M, Reineke TM. Epoxy resin thermosets derived from trehalose and  $\beta$ -cyclodextrin. *Macromolecules* 2016;49(22):8397–406.
- [3] Vidal T, Tournilhac F, Musso S, Robisson A, Leibler L. Control of reactions and network structures of epoxy thermosets. *Prog Polym Sci* 2016;62:126–79.
- [4] Raquez J, Deléglise M, Lacrampe M, Krawczak P. Thermosetting (bio) materials derived from renewable resources: a critical review. *Prog Polym Sci* 2010;35(4):487–509.
- [5] Baruah P, Karak N. Bio-based tough hyperbranched epoxy/graphene oxide nanocomposite with enhanced biodegradability attribute. *Polym Degrad Stabil* 2016;129:26–33.
- [6] Qian X, Song L, Bihe Y, Yu B, Shi Y, Hu Y, et al. Organic/inorganic flame retardants containing phosphorus, nitrogen and silicon: preparation and their performance on the flame retardancy of epoxy resins as a novel intumescent flame retardant system. *Mater Chem Phys* 2014;143(3):1243–52.
- [7] Ma S, Liu X, Jiang Y, Fan L, Feng J, Zhu J. Synthesis and properties of phosphorus-containing bio-based epoxy resin from itaconic acid. *Sci China Chem* 2014;57(3):379–88.
- [8] Yang W, Wu S, Yang W, Yuen A, Zhou Y, Guan Y, et al. Nanoparticles of polydopamine for improving mechanical and flame-retardant properties of an epoxy resin. *Compos B Eng* 2020;186:107828.
- [9] Fang F, Song P, Ran S, Wang H, Fang Z. A facile way to prepare phosphorus-nitrogen-functionalized graphene oxide for enhancing the flame retardancy of epoxy resin". *Compos Comm* 2018;10:97–102.
- [10] Peng C, Chen T, Zeng B, Chen G, Yuan C, Xu Y, et al. Anderson-type polyoxometalate-based hybrid with high flame retardant efficiency for the preparation of multifunctional epoxy resin nanocomposites. *Compos B Eng* 2020:107780.
- [11] Ma C, Yu B, Hong N, Pan Y, Hu W, Hu Y. Facile synthesis of a highly efficient, halogen-free, and intumescent flame retardant for epoxy resins: thermal properties, combustion behaviors, and flame-retardant mechanisms. *Ind Eng Chem Res* 2016;55(41):10868–79.
- [12] Carja I, Serbezeanu D, Vlad-Bubulac T, Hamciuc C, Coroaba A, Lisa G, et al. A straightforward, eco-friendly and cost-effective approach towards flame retardant epoxy resins. *J Mater Chem* 2014;2(38):16230–41.
- [13] Jian R, Wang P, Duan W, Wang J, Zheng X, Weng J. Synthesis of a novel P/N/S-containing flame retardant and its application in epoxy resin: thermal property, flame retardance, and pyrolysis behavior. *Ind Eng Chem Res* 2016;55(44):11520–7.
- [14] Dai J, Ma S, Wu Y, Han L, Zhang L, Zhu J, et al. Polyesters derived from itaconic acid for the properties and bio-based content enhancement of soybean oil-based thermosets. *Green Chem* 2015;17(4):2383–92.
- [15] Teng N, Yang S, Dai J, Wang S, Zhao J, Zhu J, et al. Making benzoxazine greener and stronger: renewable resource, microwave irradiation, green solvent and excellent thermal properties. *ACS Sustainable Chem Eng* 2019;7:8715–23.
- [16] Wang S, Ma S, Li Q, Yuan W, Wang B, Zhu J. Robust, fire-safe, monomer-recovery, highly malleable thermosets from renewable bioresources. *Macromolecules* 2018;51(20):8001–12.
- [17] Xiong Y, Zhang X, Liu J, Li M, Guo F, Xia X, et al. Synthesis of novel phosphorus-containing epoxy hardeners and thermal stability and flame-retardant properties of cured products. *J Appl Polym Sci* 2012;125(2):1219–25.
- [18] Wang X, Hu Y, Song L, Xing W, Lu H, Lv P, et al. Flame retardancy and thermal degradation mechanism of epoxy resin composites based on a DOPO substituted organophosphorus oligomer. *Polymer* 2010;51(11):2435–45.
- [19] Dai J, Teng N, Peng Y, Liu Y, Cao L, Zhu J, et al. Biobased benzoxazine derived from daidzein and furfurylamine: microwave-assisted synthesis and thermal properties investigation. *ChemSusChem* 2018;11(18):3175–83.
- [20] Pourchet S, Sonnier R, Ben A, Gaillard Y, Ruiz Q. New reactive isoeugenol based phosphate flame retardant toward green epoxy resins. *ACS Sustainable Chem Eng* 2019;7:14074–88.
- [21] Wang X, Guo W, Song L, Hu Y. Intrinsically flame-retardant bio-based epoxy thermosets: a review. *Compos B Eng* 2019:107487.
- [22] Dai J, Teng N, Liu J, Feng J, Zhu J, Liu X. Synthesis of bio-based fire-resistant epoxy without addition of flame retardant elements. *Compos B Eng* 2019;179:107523.
- [23] Sun Z, Fridrich B, de Santi A, Elangovan S, Barta K. Bright side of lignin depolymerization: toward new platform chemicals. *Chem Rev* 2018;118(2):614–78.
- [24] Liu L, Huang G, Song P, Yu Y, Fu S. Converting industrial alkali lignin to biobased functional additives for improving fire behavior and smoke suppression of polybutylene succinate. *ACS Sustainable Chem Eng* 2016;4(9):4732–42.
- [25] Ma S, Li T, Liu X, Zhu J. Research progress on bio-based thermosetting resins. *Polym Int* 2016;65(2):164–73.
- [26] Savonnet E, Grau E, Grelier S, Defoort B, Cramail H. Divanillin-based epoxy precursors as DGEBA substitutes for biobased epoxy thermosets. *ACS Sustainable Chem Eng* 2018;6(8):11008–17.
- [27] Auvergne R, Caillol S, David G, Boutevin B, Pascault J. Biobased thermosetting epoxy: present and future. *Chem Rev* 2013;114(2):1082–115.
- [28] Ma S, Liu X, Jiang Y, Tang Z, Zhang C, Zhu J. Bio-based epoxy resin from itaconic acid and its thermosets cured with anhydride and comonomers. *Green Chem* 2013;15(1):245–54.
- [29] Huang K, Ma S, Wang S, Li Q, Wu Z, Liu J, et al. Sustainable valorization of lignin with levulinic acid and its application in polyimine thermosets. *Green Chem* 2019;21(18):4964–70.
- [30] Fang F, Ran S, Fang Z, Song P, Wang H. Improved flame resistance and thermo-mechanical properties of epoxy resin nanocomposites from functionalized graphene oxide via self-assembly in water. *Compos B Eng* 2019;165:406–16.
- [31] Liu X, Zong E, Hu W, Song P, Wang J, Liu Q, Ma Z, Fu S. Lignin-derived porous carbon loaded with La(OH)3 nanorods for highly efficient removal of phosphate". *ACS Sustain Chem Chem* 2019;7(1):758–68.
- [32] Liu L, Qian M, Song P, Huang G, Yu Y, Fu S. Fabrication of green lignin-based flame retardants for enhancing the thermal and fire retardancy properties of polypropylene/wood composites. *ACS Sustainable Chem Eng* 2016;4(4):2422–31.
- [33] Peng Y, Liu Y, Dai J, Cao L, Liu X. A sustainable strategy for remediation of oily sewage: clean and safe. *Separ Purif Technol* 2020;240:116592.
- [34] Tao S. Positronium annihilation in molecular substances. *J Chem Phys* 1972;56(11):5499–510.
- [35] Feu KS, Alexander F, Silva S, de Moraes Junior MA, Corrêa AG, Paixão MW. Polyethylene glycol (PEG) as a reusable solvent medium for an asymmetric organocatalytic Michael addition. Application to the synthesis of bioactive compounds. *Green Chem* 2014;16(6):3169–74.
- [36] Shanab K, Neudorfer C, Schirmer E, Spreitzer H. Green solvents in organic synthesis: an overview. *Curr Org Chem* 2013;17(11):1179–87.
- [37] Anastas P, Eghba N. Green chemistry: principles and practice. *Chem Soc Rev* 2010;39:301–12.
- [38] Dai J, Peng Y, Teng N, Liu Y, Liu C, Shen X, et al. High-performing and fire-resistant biobased epoxy resin from renewable sources. *ACS Sustainable Chem Eng* 2018;6(6):7589–99.
- [39] Shen X, Liu X, Dai J, Liu Y, Zhang Y, Zhu J. How does the hydrogen bonding interaction influence the properties of furan-based epoxy resins. *Ind Eng Chem Res* 2017;56(38):10929–38.
- [40] Kissinger HE. Reaction kinetics in differential thermal analysis. *Anal Chem* 1957;29:1702–6.
- [41] Ozawa T. A new method of analyzing thermogravimetric data. *Bull Chem Soc Jpn* 1965;38(11):1881–92.
- [42] Xiang H, Ling H, Wang J, Song L, Gu Y. A novel high performance RTM resin based on benzoxazine. *Polym Compos* 2005;26(5):563–71.
- [43] Dai J, Na T, Shen X, Yuan L, Cao L, Jin Z, et al. Synthesis of bio-based benzoxazines suitable for vacuum assisted resin transfer molding (RTM) process via introduction of soft silicon segment. *Ind Eng Chem Res* 2018;57(8):3091–102.
- [44] Jing L, Zhang C, Liang R, Wang B. Statistical characterization and robust design of RTM processes. *Compos Part A* 2005;36(5):564–80.

- [45] Xu Y, Shi X, Lu J, Qi M, Guo D, Chen L, et al. Novel phosphorus-containing imidazolium as hardener for epoxy resin aiming at controllable latent curing behavior and flame retardancy. *Compos B Eng* 2020;184:107673.
- [46] Artner J, Ciesielski M, Walter O, Döring M, Perez RM, Sandler JKW, et al. A novel DOPO-based diamine as hardener and flame retardant for epoxy resin systems. *Macromol Mater Eng* 2010;293(6):503–14.
- [47] Hsiue G, Wei H, Shiao S, Kuo W, Sha Y. Chemical modification of dicyclopentadiene-based epoxy resins to improve compatibility and thermal properties. *Polym Degrad Stabil* 2001;73:309–18.
- [48] Altaweel AM, Ravikumar H, Ranganathaiah C. Influence of free volume on the mechanical properties of epoxy based composites: a correlation study. *Phys Status Solidi C* 2009;6(11):2401–3.
- [49] Algers J, Maurer F, Eldrup M, Wang J-S. Free volume and mechanical properties of Palacos® R bone cement. *J Mater Sci Mater Med* 2003;14(11):955–60.
- [50] Shantarovich V, Kevdina I, Yampolskii YP, Alentiev AY. Positron annihilation lifetime study of high and low free volume glassy polymers: effects of free volume sizes on the permeability and permselectivity. *Macromolecules* 2000;33(20):7453–66.
- [51] Artner J, Ciesielski M, Walter O, Döring M, Perez RM, Sandler JKW, et al. A Novel DOPO-based diamine as hardener and flame retardant for epoxy resin systems. *Macromol Mater Eng* 2010;293(6):503–14.
- [52] Schartel B, Balabanovich A, Braun U, Knoll U, Artner J, Ciesielski M, et al. Pyrolysis of epoxy resins and fire behavior of epoxy resin composites flame-retarded with 9, 10-dihydro-9-oxa-10-phosphaphenanthrene-10-oxide additives. *J Appl Polym Sci* 2007;104(4):2260–9.
- [53] Bao C, Guo Y, Yuan B, Yuan H, Lei S. Functionalized graphene oxide for fire safety applications of polymers: a combination of condensed phase flame retardant strategies. *J Mater Chem* 2012;22(43):23057–63.
- [54] Kim M, Ko H, Park S. Synergistic effects of amine-modified ammonium polyphosphate on curing behaviors and flame retardation properties of epoxy composites. *Compos B Eng* 2019;170:19–30.
- [55] Chao W, Wu Y, Li Y, Qian S, Guo Z. Flame-retardant rigid polyurethane foam with a phosphorus-nitrogen single intumescent flame retardant. *Polym Adv Technol* 2017;29(1).
- [56] Wang Z, Liu Y, Li J. Regulating effects of nitrogenous bases on char structure and flame retardancy of polypropylene/intumescent flame retardant composites. *ACS Sustainable Chem Eng* 2017;5(3):2375–83.
- [57] Wan J, Gan B, Li C, Molina-Aldareguia J, Kalali EN, Wang X, et al. A sustainable, eugenol-derived epoxy resin with high biobased content, modulus, hardness and low flammability: synthesis, curing kinetics and structure–property relationship. *Chem Eng J* 2016;284:1080–93.
- [58] Carja I, Serbezeanu D, Vlad-Bubulac T, Hamciuc C, Coroaba A, Lisa G, et al. A straightforward, eco-friendly and cost-effective approach towards flame retardant epoxy resins. *J Mater Chem* 2014;2(38):16230–41.
- [59] Zhang W, Li X, Yang R. Study on flame retardancy of TGDDM epoxy resins loaded with DOPO-POSS compound and OPS/DOPO mixture. *Polym Degrad Stabil* 2014;99:118–26.